

Ground vs. Surface Air Temperature Trends: Implications for Borehole Surface Temperature Reconstructions

Michael E. Mann

Department of Environmental Sciences, University of Virginia, Charlottesville, VA

Gavin A. Schmidt

NASA Goddard Institute for Space Studies and Center for Climate Systems Research, Columbia University, New York, NY

Abstract. We have analyzed the relationship between surface air temperature (SAT), ground surface temperature (GST), and snow cover (SNC) over the terrestrial Northern Hemisphere based on general circulation model (GCM) simulations using GISS modelE forced with the observed SST and radiative forcing changes from 1951-1998. While SAT is the dominant influence on GST during the warm-season, it explains only half of the variance in GST during the cold-season, with SNC and pre-conditioning by prior warm-season SAT also exhibiting a sizeable and, in places, dominant influence. During a period of coincident surface warming and cold-season snowcover decrease in the model (1971-1998), mean GST increases are 0.2°C less than those in SAT, a consequence of greater exposure of the ground surface to winter cold air outbreaks. Interpretations of past SAT trends from borehole-based GST reconstructions may therefore be substantially biased by seasonal influences and snow cover changes.

1. Introduction

A complex relationship exists between variations in surface air temperature (SAT) and the temperatures of the underlying ground surface (GST) in terrestrial regions. While SAT variations are driven largely by atmospheric variability, GST is in addition significantly impacted by land-surface and soil properties, vegetation, latent heat sources and sinks, and permafrost distortion [e.g., Beltrami, 1996]. In the cold season, the effects of insulating seasonal snow cover are of primary importance. Understanding how such processes may influence GST changes is important, for example, for understanding changes in the terrestrial carbon cycle in both the future [Stocker et al, 2001] and past [Gerber et al, 2002]. Important apparent discrepancies, moreover, exist between estimates of past surface temperatures from GST estimates derived from terrestrial borehole data, and those derived from other paleoclimate proxy data [Huang et al, 2000; Harris and Chapman, 2001; Folland et al, 2001; Briffa and Osborn, 2002; Mann et al, 2003]. It has recently been suggested [Mann et al, 2003] that differences between proxy-based SAT estimates and borehole-derived GST estimates in past centuries may in large part be explained by the influence of cold-season snow cover on GST in the extratropical regions from which most of the borehole estimates are obtained. Such a bias would imply greater sensitivity of borehole-based SAT estimates to warm-season temperature variations. Moreover, changes in the extent and duration of seasonal snow cover will potentially introduce a time-dependence to this seasonal sampling bias. Evaluating these factors requires an investigation of the processes impacting GST variations and the differences between SAT and GST trends over time.

To investigate such factors, we make use of a climate model simulation of the latter half of the 20th century employing the GISS modelE GCM [Schmidt et al, 2003] which includes large-scale climate forcing, realistic atmospheric variability, snow hydrology, and a representation of surface, vegetation, and sub-surface thermal properties. In the real world, there are further effects that may compromise the interpretation of GST estimates derived from terrestrial borehole data. These include anthropogenic land use changes in particular [e.g. Skinner and Majorowicz, 1999], but also small-scale heterogeneity in soil, land-surface and microclimatic influences [Gosnold et al, 1997] and the complicating influence of geothermal heat flux [e.g., Harris and Chapman, 1997]. Within a climate model simulation, we are able to analyze a 'best case' scenario, in which these complicating factors are not present. Thus any differences found in the model simulations are due entirely to physical differences between the response of GST and SAT to model-generated climate variability. For this reason, discrepancies between actual GST and SAT estimates are almost certain to be greater than those isolated in the simulation examined here.

2. Model Description

The horizontal resolution of the model is $4^\circ \times 5^\circ$ and has 18 layers in the vertical. The physics in the model is similar to that described in Hansen et al [2002]. The land surface model consists of 6 soil layers of varying thickness calculated separately for bare and vegetated ground [Rosenzweig and Abramopolous, 1997]. The vegetation type and fraction is fixed from present day observations [Matthews, 1984]. The snow model is a 3-layer formulation which allows for a varying snow-covered fraction and water percolation [Stieglitz, 1994]. We define GST as the temperature of the uppermost vegetated soil layer, SAT as the surface air temperature (defined as 10m up in this model--variations at e.g. 2m are the same), and SNC is the mean fraction of snow cover in the grid box (mean snow depth also co-varies closely with SNC at seasonal timescales). The forcings applied to the model over the period 1950-1998 are the observed sea surface temperatures and sea ice conditions, variations in well-mixed greenhouse gases, stratospheric ozone, volcanic aerosols, tropospheric ozone, stratospheric water vapor and solar irradiance (as described in Hansen et al [2002]). Global mean temperature trends over this period are well captured by the model. However, regional patterns of climate change (including those in snowcover) differ from observations, particularly since the model does not exhibit any long-term trend in the Northern Hemisphere winter circulation indices [Thomson and Wallace, 2001]. Nonetheless, the modeled relationships between SAT, GST, and SNC are likely to be representative of their real-world analogues.

3. Results

We focus on the extratropical terrestrial region of the Northern Hemisphere (latitudes greater than 30°N) since this is, for example, the domain over which the vast majority of borehole-based GST estimates come from [e.g. Huang et al, 2000; Harris and Chapman, 2001]. We analyze separately cold-season (Oct-Mar) and warm-season (Apr-Sep) half years. Figure 1 compares the mean extratropical Northern Hemisphere SAT and GST during the two half-year seasons. GST is observed to track concurrent SAT remarkably closely

during the warm-season. By contrast, significant differences between the two quantities are observed during the cold-season. A positive correlation of cold-season GST with cold-season SAT ($r=0.9$) is observed, as is a negative correlation with cold-season snow cover ($r=-0.6$), and a substantial positive correlation ($r=0.7$) with prior warm-season SAT. An association between cold-season GST and prior warm-season SAT is consistent with the preservation of warm-season atmospheric influence due to insulating cold-season snow cover. Cold-season snow cover provides an additional influence on cold-season GST, modulating the exposure of the cold-season ground surface to concurrent cold-season SAT variations.

An appropriate statistical model for cold-season GST (G_c) variability thus must consider, at a minimum, the multiple predictors of concurrent cold-season SAT (T_c), cold-season SNC (S_c), and prior warm-season SAT (T_w). There is a clear co-linearity of the predictors at the hemispheric mean scale, each of which exhibit strong trends during the past three decades (patterns of trend shown in Figure 2; mean G_c increase is 0.85°C , mean T_c increase is 1.0°C , mean winter S_c decrease is 2% areal coverage). Thus it is not possible to determine the relative influences of T_c , T_w , and S_c on G_c simply from a comparison of the hemispheric mean time series. For example, the decrease in recent decades in areal-mean S_c is likely a result of increased T_c , and it is thus not possible to simultaneously determine the additional, more subtle, influence of decreases in S_c on G_c from hemispheric mean trends alone.

To separate the partial influences of T_c , S_c , and T_w on G_c , we performed a multivariate linear regression at each model grid box using the full 48 years of data available from the model simulation,

$$G_c(\phi, \lambda) = \alpha T_c(\phi, \lambda) + \beta S_c(\phi, \lambda) + \gamma T_w(\phi, \lambda) + \varepsilon \quad (1)$$

where ϕ, λ refer to the central latitude and longitude of each model grid box. The predictors and predictand were standardized prior to the regression, so that α, β , and γ are partial standardized regression coefficients which specify the partial influence of each of the three predictors, and ε is an assumed white noise error term. Standard errors were determined for all regression coefficients.

This analysis yields an areally-weighted mean estimate over the Northern Hemisphere domain analyzed of $\alpha=0.70$, $\beta=0.4$, $\gamma=0.14$, which are in the mean significant at the $p=0.01$, 0.03 , and 0.11 levels respectively (based on a one-sided null hypothesis, since positive relationships between each of the three predictors and the predictand are dictated by physical considerations; G_c can be assumed to vary positively with T_c , and T_w , and also with S_c since increased snow cover provides greater insulation against cold air outbreaks). T_c plays a surprisingly modest role in explaining G_c variations over the period analyzed, resolving less than half (48%) of the total variance therein. S_c variations resolve an additional 9% and T_w 4% of the total variance in G_c indicating less important, but still significant explanatory roles at the hemispheric mean scale. The combined variance explained by the three predictors is 61%. By contrast, a parallel analysis for the warm-season indicates that a majority of the variance in GST (78%) is resolved by the single predictor of concurrent warm-

season SAT alone. Additional factors not explicitly considered in our analysis, such as soil moisture effects, latent heat considerations and permafrost changes at higher latitudes, must be responsible for the sizeable residual unexplained variance in G_c . It is also possible that the influences of S_c and perhaps T_w are underestimated by the approximation of linear relationships assumed in the regression analysis, and that the subtle seasonal influences of snowcover on GST may not entirely be captured with cold-season and warm-season half year relationships.

The regression coefficients α , β and γ were used to project the components of the 1971-1998 trend in G_c (Figure 2a) associated with T_c , S_c and T_w respectively (Figure 3). Consistent with the results of the multivariate regression, the dominant factor is changes in T_c which resolve, in the areally-weighted domain mean, 0.65°C of the 0.85°C increase in areally-weighted domain mean G_c , with the pattern of T_c warming similar to, but damped relative to, that for G_c . By contrast, S_c changes (which in most regions are sizeable, see Figure 2d) impart an areal-mean G_c cooling trend of 0.2°C. The greatest cooling influence, not surprisingly, is evident in regions (e.g. higher latitudes of North America and Tibetan plateau) where greatest decrease in S_c are observed (Figure 2d). The close correspondence between the spatial pattern of available borehole temperature estimates [e.g. Huang et al, 2000] and the pattern evident in Figure 2d suggests that the influence of snowcover changes could be especially large in hemispheric estimates formed from the sparse available borehole measurements. An estimated 0.12°C areal-mean warming trend in G_c is associated with T_w with greatest apparent influence found, as we would expect, at higher latitudes and elevations where mean cold-season snow cover is greatest. These three influences therefore resolve in combination roughly 0.6°C of the observed hemispheric mean 0.85°C G_c increase. This leaves 0.25°C of the mean warming unexplained (at least, in a linearly additive) sense, by the factors analyzed.

4. Conclusions

Analysis of a forced climate model simulation employing physically-based representations of land-surface, ground, and hydrological processes indicates that ground surface temperature in the Northern Hemisphere closely tracks surface air temperature only during the warm-season. During the cold-season, snow cover provides an insulating influence of the ground surface from SAT variations. This serves both to exaggerate the influence of warm-season SAT on annual GST variations, and to provide a source of bias in interpreting SAT changes from GST changes, in the face of changing snow cover. Other factors (such as soil moisture changes, seasonal latent heat absorption and/or release, or non-linear interactions between predictors) may also be necessary to explain the remaining variance in cold-season GST variations unresolved by any of the predictors considered in our analysis. We feel that the results of our modeling study are likely to be representative more generally to continental-scale climate changes over the past few centuries.

Proxy-based hemispheric SAT reconstructions indicate roughly 0.2-0.3°C less cooling (relative to modern) during the depths of the so-called Little Ice Age or 'LIA' (e.g., the 16th-17th centuries) than do appropriate hemispheric mean GST

estimates from borehole data [Briffa and Osborn, 2002; Mann et al, 2003]. This difference is reduced essentially to zero when an optimal borehole 'SAT' estimate is determined by eliminating the projections of spatial patterns of variance in the borehole GST estimates that are statistically inconsistent with the instrumental SAT record during the 20th century [and thus indicative of non-SAT related bias--see Mann et al, 2003]. It has been argued that modern land use changes, a factor absent in our model simulation, contribute such a pattern of bias, imparting an anomalous component of 20th century warming in borehole GST estimates over a large part of North America [Skinner and Majorowicz, 1999]. This anomalous GST warming would indeed lead to artificially cold 'LIA' temperature estimates from boreholes, since the borehole estimates of past temperature change are defined relative to a late 20th century GST baseline assumed equal to that of the instrumental SAT record [e.g. Huang et al, 2000; Mann et al, 2003].

The current study suggests that another contributing factor may be the bias inherent in the seasonal sensitivity of GST to SAT variations in the presence of seasonal snowcover. Initial modeling studies suggest less continental precipitation in the 'LIA' owing to a less intense hydrological cycle [Bauer et al, 2003]. The negative phase of the North Atlantic Oscillation (NAO) atmospheric circulation pattern that has been inferred for the 'LIA' [e.g. Shindell et al, 2002] implies a further reduction in winter continental precipitation. Whether or not such changes translate to decreased continental snowcover is, at present, unclear, though long-term transient climate model runs should provide further insight. However, if such changes in snowcover have occurred, they imply anomalous cooling of GST relative to SAT in earlier centuries. The considerable spatial variability in the amplitude of snow cover influences on cold-season GST suggests, moreover, the added likelihood of spatial sampling bias in the estimation of past hemispheric-mean SAT histories from the regionally-sparse available borehole GST estimates.

Acknowledgments. M.E.M. acknowledges support for this work through a sabbatical leave from the University of Virginia and support at host institution NASA Goddard Institute for Space Studies provided by the NASA Goddard Space Flight Center. Climate modeling at GISS is supported by NASA.

References

- Beltrami, H., Active Layer Distortion of Annual Air/Soil Thermal Orbits: Permafrost and Past Climates, *Permafrost and Periglacial Processes*, 7, 101-110, 1996.
- Bauer E., M. Claussen, A. Hunebein, V. Brovkin, in *The KIHZ Project: Towards a Synthesis of Paleoclimate Variability Using Proxy Data and Climate Models*, H. Fischer et al., Eds. (Springer-Verlag, Berlin, in press).
- Briffa, K.R., and T. J. Osborn, Blowing Hot and Cold, *Science*, 295, 2227-2228, 2002.
- Gerber, S., F. Joos, P. Brügger, T. F. Stocker, M. E. Mann, S. Sitch, and M. Scholze, Constraining temperature variations over the last millennium by comparing simulated and observed atmospheric CO₂, *Climate Dynamics*, 20, 281-299, 2003.
- Gosnold, W. D. Jr., P.E. Todhunter, and W.L. Schmidt, The borehole temperature record of climate warming in the mid-continent of North America, *Global and Planetary Change*, 15, 33-45, 1997.
- Hansen, J., M. Sato, L. Nazarenko, R. Ruedy, A. Lacis, D. Koch, I. Tegen, T. Hall, D. Shindell, P. Stone, T. Novakov, L. Thomason, R. Wang, Y. Wang, D.J. Jacob, S. Hollandsworth-Frith, L. Bishop, J. Logan, A. Thompson, R. Stolarski, J. Lean, R. Willson, S. Levitus, J. Antonov, N. Rayner, D. Parker, and J. Christy,

- Climate forcings in Goddard Institute for Space Studies SI2000 simulations. *J. Geophys. Res.* 107 (D18), 4347, doi: 10.1029/2001JD001143, 2002.
- Harris, R. N., and D. S. Chapman, Borehole temperatures and a baseline for 20th-century global warming estimates, *Science*, 275, 1618-1621, 1997.
- Harris, R. N., and D. S. Chapman, Mid-Latitude (30'-60' N) climatic warming inferred by combining borehole temperatures with surface air temperatures, *Geophys. Res. Lett.* 28, 747-750, 2001.
- Huang, S., H. N. Pollack and P.-Y. Shen, Temperature Trends Over the Past Five Centuries Reconstructed from Borehole Temperature, *Nature* 403, 756-758, 2000.
- Mann, M.E., S. Rutherford, R.S. Bradley, M.K. Hughes, and F.T. Keimig, Optimal Surface Temperature Reconstructions Using Terrestrial Borehole Data, *J. Geophys. Res.*, in press, 2003
- Mathews, E., Prescription of Land-Surface Boundary Conditions in GISS GCM II: A Simple Method Based on High-Resolution Vegetation Data Bases. NASA TM-86096. National Aeronautics and Space Administration. Washington, D.C. 1984
- Rosenzweig, C., and F. Abramopoulos, Land-surface model development for the GISS GCM, *J. Climate*, 10, 2040-2054, 1997.
- Schmidt, G. A., J. E. Hansen, R. Ruedy, I. Alienov, Y. Cheng, M. S. Yao, A. D. Del Genio and D. Rind, Climatology of the GISS ModelE simulations. (in preparation).
- Shindell, D.T., G.A. Schmidt, M.E. Mann, D. Rind, and A. Waple, A., Solar forcing of regional climate change during the Maunder Minimum, *Science*, 294, 2149-2152, 2001.
- Skinner, W. R. and J. A. Majorowicz, Regional climatic warming and associated twentieth century land-cover changes in north-western North America. *Climate Research*, 12, 39-52, 1999.
- Stocker, T. F., G.K.C. Clarke, H. Le Treut, R.S. Lindzen, V.P. Meleshko, R.K. Mugara, T.N. Palmer, R.T. Pierrehumbert, P.J. Sellers, K.E. Trenberth, J. Willebrand, Physical Climate Processes and Feedbacks, in *Climate Change 2001: The Scientific Basis*, Houghton, J.T., et al. (eds.), Cambridge Univ. Press, Cambridge, 695-738, 2001.
- Thompson, D.W.J., and J.M. Wallace, Regional Climate Impacts of the Northern Hemisphere Annular Mode, *Science*, 293, 85-89, 2001.

M. E. Mann, Department of Environmental Sciences, University of Virginia, Charlottesville, VA 22902. (email: mann@virginia.edu)
 G. A. Schmidt, NASA GISS and Center for Climate Systems Research, 2880 Broadway, New York, NY 10025 (email: gschmidt@giss.nasa.gov)

MANN AND SCHMIDT: GROUND VS. SURFACE AIR TEMP. TRENDS
 MANN AND SCHMIDT: GROUND VS. SURFACE AIR TEMP. TRENDS
 MANN AND SCHMIDT: GROUND VS. SURFACE AIR TEMP. TRENDS

Figure 1. Comparison of hemispheric mean SAT, GST and SNC series (anomalies relative to 1951-1998 means). Shown are comparisons of (a) warm-season GST (blue) and warm-season SAT (red), (b) cold-season GST (blue), cold-season SAT (red) and (negative) cold-season SNC (green). Scales for GST and SAT are °C (right vertical axis) and scale for SNC is in % change (left vertical axis).

Figure 2. Spatial patterns of 1971-1998 trends in (a) cold-season GST (G_c), (b) cold-season SAT (T_c), (c) the difference ($T_c - G_c$), and (d) cold-season SNC (S_c). Color scale indicates trend in °C.

Figure 3. Spatial patterns of components of 1971-1998 G_c trend (Figure 2a) associated with (a) T_c , (b) S_c and (c) T_w . Color scale indicates trend in °C.

FIGURE 1

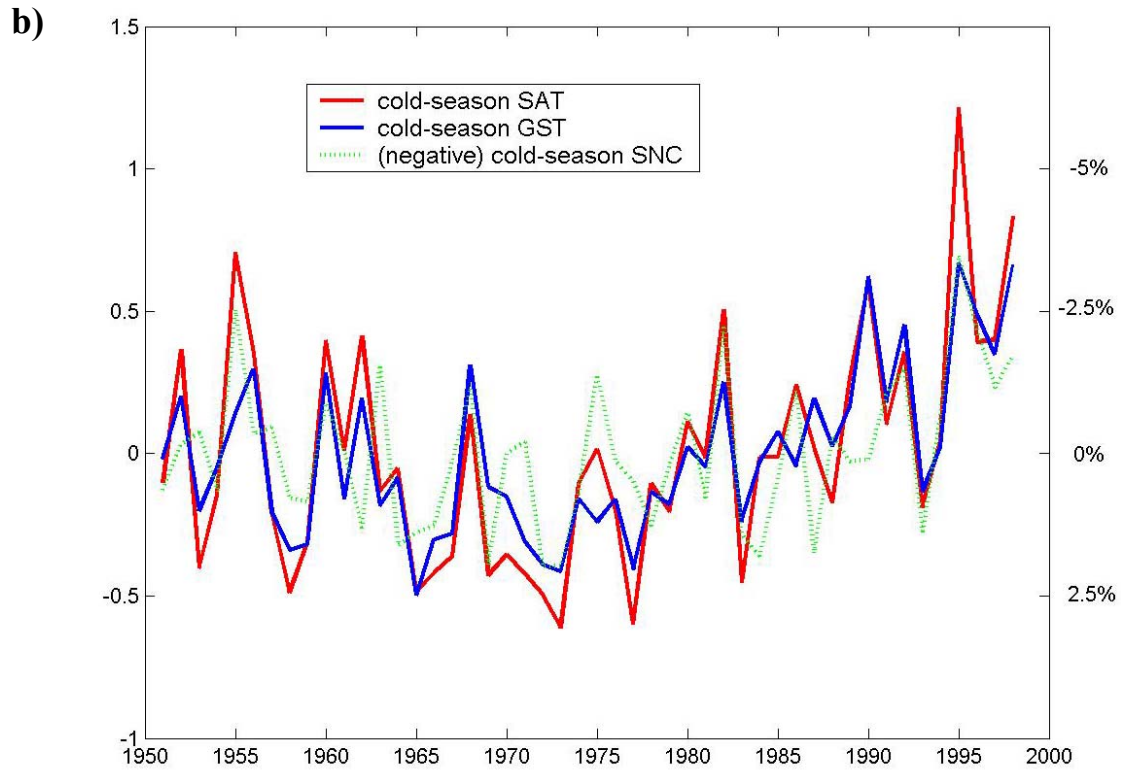
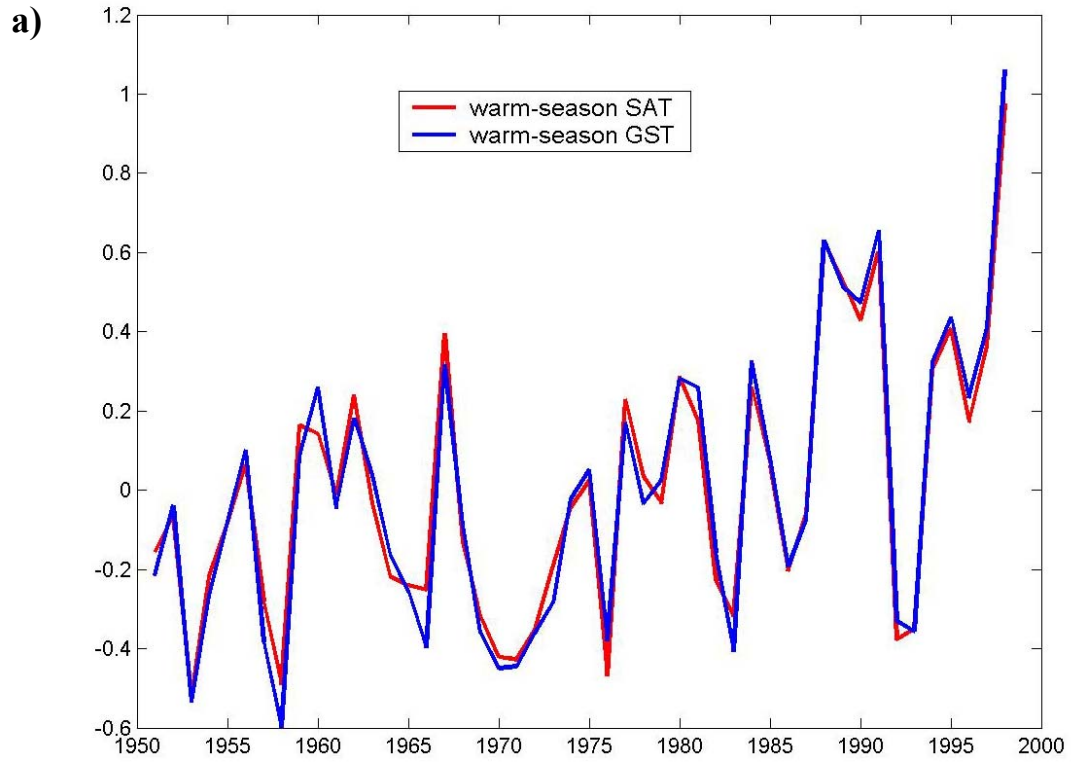


FIGURE 2

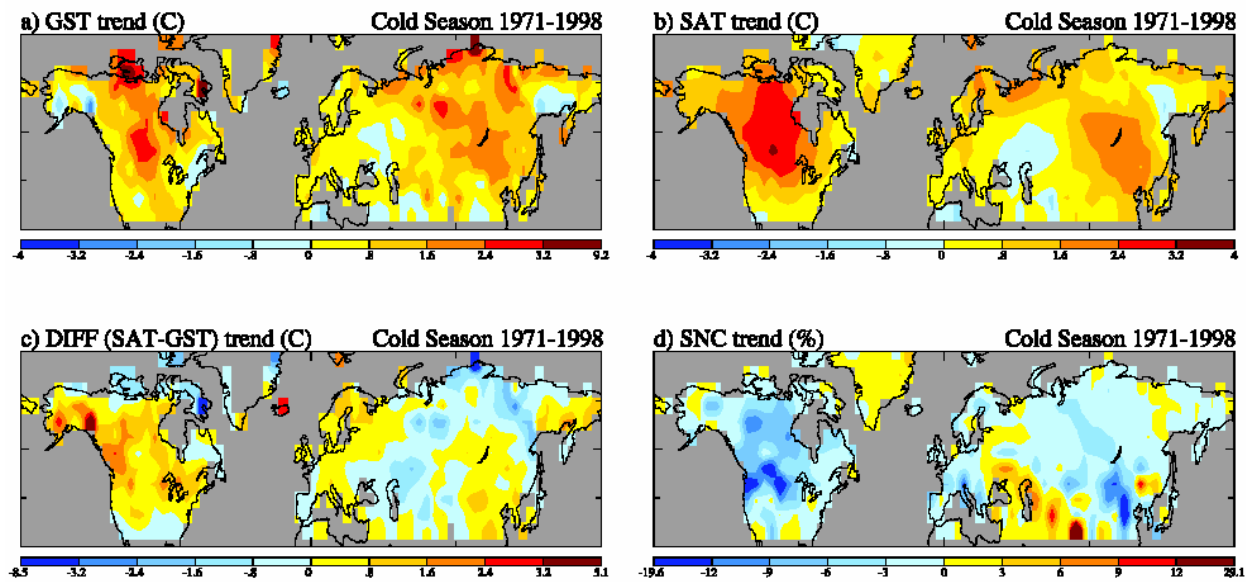


FIGURE 3

